Title
Electron trapping non-uniformity in high-pressure-Bridgman-grown CdZnTe

Journal
Journal of Applied Physics, 92(6)

Authors
Amman, Mark
Lee, Julie S.
Luke, Paul N.

Publication Date
2002-05-09

Electron trapping non-uniformity in high-pressure-Bridgman-grown CdZnTe

Mark Amman, Julie S. Lee, and Paul N. Luke
Ernest Orlando Lawrence Berkeley National Laboratory
University of California, Berkeley, California 94720

ABSTRACT

Gamma-ray spectroscopy is a valuable tool of science and technology. Many applications for this tool are in need of a detector technology capable of achieving excellent energy resolution and efficient detection while operating at room temperature. Detectors based on the material cadmium zinc telluride (CdZnTe) could potentially meet this need if certain material deficiencies are addressed. The coplanar-grid as well as other electron-only detection techniques are effective in overcoming some of the material problems of CdZnTe and, consequently, have led to efficient gamma-ray detectors with good energy resolution while operating at room temperature. At the present time, the performance of these detectors is mainly limited by the degree of uniformity in electron generation and transport. Despite recent progress in the growth of CdZnTe material, small variations in these properties remain a barrier to the widespread success of such detectors. Alpha-particle response characterization of CdZnTe crystals fabricated into simple planar detectors provides an effective tool to accurately study such variations. We have used a finely collimated alpha source to produce two-dimensional maps of detector response. For a number of crystals, a clear correlation has been observed between their alpha response maps and the distribution of tellurium inclusions inside the crystals. An analysis of the induced charge signals indicates that regions of enhanced electron trapping are associated with the inclusions, and that these regions extend beyond the physical size of the inclusions. Such regions introduce non-uniform electron trapping in the material that then degrades the spectroscopic performance of the material as a gamma-ray detector.

I. INTRODUCTION

Gamma-ray spectroscopy is an extremely powerful tool for the identification and characterization of nuclear materials and interactions. A large and diverse set of application areas exists including astronomy, nuclear physics, weapons safeguards and nonproliferation, and environmental remediation. Detectors in the form of large-volume reverse-biased germanium (Ge) diodes are almost exclusively used in applications requiring high-resolution spectroscopy and good detection efficiency. Unfortunately, the small band gap of Ge necessitates cooling to temperatures typically less than 100 K in order to reduce thermally generated charge carriers that would degrade the signal-to-noise ratio. This cooling requirement and the associated bulk and complexity of a cryostat enclosure make this technology prohibitively expensive or impractical for many applications. A highly sought goal then is a wide bandgap semiconducting material with the properties required to produce detectors that operate at or near room temperature and that approach the energy resolution and efficiency of Ge-based gamma-ray detectors. One candidate material to meet this need is cadmium zinc telluride (CdZnTe). The potential of CdZnTe has been demonstrated through many material and detector technology developments over the last decade.[1-13] The material has the desirable intrinsic properties of a wide bandgap necessary for room-temperature operation and a high average atomic number for efficient gamma-ray stopping. Furthermore, the CdZnTe material that is commercially available today exhibits negligible polarization effects, has a high bulk resistivity, and has reasonably good electron collection properties.[14] The material, however, continues to suffer from poor hole transport leading to large-volume detectors with poor spectroscopic performance when conventional detection techniques are used. Consequently, techniques in which the detector signal is almost exclusively derived from electron collection have become the most viable approaches for the successful application of CdZnTe to high-efficiency gamma-ray detection when good energy resolution is required. One of these *electron-only* approaches is the coplanar-grid charge-sensing technique.[5] This technique and its variations offer the advantages of nearly eliminating the hole collection problem, providing accurate and adjustable correction for electron trapping, producing uniform charge induction,[15,16] realizing near full-volume detection efficiency,[17,18] and requiring only simple conventional pulse-processing electronics. Coplanar-grid detectors 1cm^3 in size have achieved energy resolutions down to about 2% FWHM at 662keV, and hand-held systems have been produced from such detectors.[18]

Despite the accomplishments of the coplanar-grid and other electron-only techniques, the widespread application of CdZnTe remains hampered by the poor availability of large crystals with the uniformity required to achieve good energy resolution. Critical to the success of electron-only devices is spatial uniformity in both the quantity of electron charge generated by gamma rays and the electron transport within the CdZnTe material. It is now well established that randomly-oriented grain boundaries can cause severe electron trapping and thereby substantially degrade the spectroscopic performance of these devices.[14,19-21] For this reason, crystals free of these grain boundaries must be selectively cut from the polycrystalline ingots typically produced. Once these grain boundaries and other large-scale crystal defects such as cracks are eliminated through this selection process, small inhomogeneities in the electron generation and transport properties of the material remain. These small variations then typically limit the performance of the electron-only detectors produced from the material. The average level of the electron transport (as characterized by the electron mobility-lifetime product) achieved today in commercially produced material is not limiting detector performance and is sufficient to achieve good energy resolution with techniques such as the coplanar grid. It is the spatial variations in electron transport and electron generation that are presently the primary material problem. Therefore, it has now become essential to identify the fundamental causes of these variations and then use this information to improve the growth of the material.

We have used alpha-particle response measurements to characterize these electron generation and transport variations.[22-24] In one such method, an alpha-particle source is used to probe the cathode side of a CdZnTe crystal that has been fabricated into a simple planar detector. Each alpha-particle interaction event in the detector generates a well-defined number of electron-hole pairs near the cathode. The collection of this charge produces an induced charge pulse on the detector electrodes that is almost entirely determined by the electron generation at the cathode and by the transport of the electrons through the entire detector thickness. Non-uniformity in these properties is reflected in the alpha-response measurements as variations in the signal pulses. The extent of the non-uniformity can be assessed by accumulating pulse-height spectra, and the nature of the non-uniformity can be determined by comparing the shapes of individual induced charge signal pulses. By finely collimating the alpha-particle source and performing these analyses as a function of location along the cathode, spatial maps of the material can be obtained. We have made such measurements on commercially available CdZnTe crystals and have compared them to infrared transmission images of these same crystals. In this paper we discuss these measurements and show evidence of a positive correlation between the presence of large (20 - 30 μm diameter) tellurium inclusions and the degradation of the alpha-particle response. This finding is significant since the gamma-ray detector-grade CdZnTe produced today typically contains large concentrations of tellurium inclusions.[25] Through an analysis of the induced charge signals, we discover that the non-uniformity in detector response is a result of enhanced electron trapping in the vicinity of the inclusions. For several crystals studied, this appears to be the dominant non-uniformity affecting the crystal performance as a gamma-ray detector.

In the remainder of the paper, we first describe the fabrication process used to prepare the CdZnTe crystals for characterization and then give the details of the alpha-particle response characterization technique. Following this, we present and discuss the alpha response measurements and their relationship to defects identified through infrared transmission microscopy. Finally, we end with a summary of the paper.

II. CHARACTERIZATION PROCEDURE

The results presented in this paper are from CdZnTe material grown using the high-pressure Bridgman (HPB) method by eV Products.[26] For this study, a standard crystal geometry in the form of a cube approximately 1 cm^3 in size was chosen as a compromise between the desire for large volumes and the need for reasonable quantities of crystals free from random grain boundaries. This standardization of the sample geometry and the testing procedure to be described later is essential for evaluating and comparing different CdZnTe crystals and for tracking the progress made over time in the production of the material.

The usefulness of alpha-particle response measurements can depend on the detector fabrication process and the characterization procedure as well as on the material properties themselves. For this reason, the details of both the detector fabrication and the alpha characterization are given here. The processing of each CdZnTe crystal consists first of lapping the crystal surfaces with a fine-grit alumina powder in water slurry on a glass plate. The scattering of light from the lapped crystal surfaces is dependent on the crystallographic orientation thereby allowing the identification of grain boundaries through simple visual inspection of the surfaces. We crudely categorize a boundary as either a *twin* if it is straight or *random* if it is not. The typically large electron trapping problems associated with random boundaries are well documented,[19] and nearly all of the crystals that we tested with such boundaries led to coplanar-grid detectors with gamma-ray detection performance problems that included substantial background counts, poor energy resolution, and poor photopeak efficiency. In contrast, the presence of twin grain boundaries typically does not directly lead to poor coplanar-grid gamma performance, although they sometime cause electron transport non-uniformities and produce slight degradation in coplanar-grid energy resolution.[23] Because of the well-established degradation effects of random grain boundaries, the results in this paper are from crystals that have either no visible grain boundaries or only twin boundaries.

Following the lapped surface inspection, the crystal is mechanically polished with a water-based slurry of sub-micron alumina powder on a polishing pad in order to produce smooth surfaces. The crystal is then characterized using infrared transmission microscopy through which pipes, precipitates, and inclusions are identified. The fabrication of the crystal into a simple planar detector is continued by chemically etching the crystal in an approximately 2 % bromine-methanol solution in order to remove the surface damage introduced by the mechanical processing. Immediately following the etch, full-area gold electrodes approximately 80 - 90 nm thick are deposited onto two opposing detector surfaces through thermal evaporation. The completed planar detector is then placed into a vacuum chamber where the alpha-particle response measurements are made.

The measurement configuration for the alpha-particle characterization of the planar-geometry CdZnTe detector is illustrated in Fig. 1. In this technique, one of the detector electrodes is illuminated with alpha particles from an ^{241}Am source. Each alpha particle that enters the detector deposits its energy within about 20 μm of the entrance electrode[27] thereby generating in the CdZnTe electron-hole pairs very near the electrode surface. The amount of this generated charge is proportional to the deposited energy. A bias is applied across the detector to collect the electrons and holes generated by each alpha-particle interaction event. As the charge drifts and separates, charge is induced on the detector electrodes and is measured with a charge-sensitive preamplifier. Each interaction event produces a distinct induced charge pulse that is then shaped with a shaping amplifier. The pulse height of the resultant shaped pulse is then extracted and binned in the multi-channel analyzer (MCA). In an ideal radiation detector, the measured pulse height is directly proportional to the generated charge and consequently the energy deposited by the interacting particle. The accumulated counts in the MCA will then form an energy spectrum of the incident particles. For the measurements of interest here, a thin windowless alpha source is used, and the measurements are made under vacuum to ensure that the alpha particles entering the detector have a narrow energy distribution. Consequently, any excessive amount of pulse-height variation observed will be predominantly a result of deficiencies in the detector material. Effects due to the electrical contact and the near-contact region are found to be negligible in these measurements, as discussed below. For electron-only type devices, the electron generation at the radiation interaction site and the electron transport through the crystal are of primary concern. For this reason, the alpha source is used to probe the cathode of the CdZnTe crystal, as shown in Fig. 1. In this configuration, the generated holes are readily collected by the cathode and contribute practically nothing to the detected signal. Whereas, the electrons drift through the entire crystal length thereby producing the induced charge pulses measured at the anode.

Using this configuration, the overall electron generation and transport uniformity of a crystal is characterized. This is accomplished by uniformly illuminating the full cathode area of the crystal with the uncollimated ^{241}Am alpha-particle

source and measuring the resultant pulse-height spectrum at a typical detector bias of 1000 V. The spectral line shape and any background that may be present provide a measure of uniformity.

Once the overall level of uniformity of a crystal is established through the full-area alpha-particle response, we investigate the nature of the inhomogeneities using alpha-particle scanning. For this measurement, the alpha source is collimated to produce a beam diameter of about 300 μm, and the source is mounted on a scanning stage. In this way, the beam can be positioned anywhere along the cathode, and only a very small region of the CdZnTe crystal is probed at a time. LabVIEW code is used to control the stage scanning and the acquisition of pulse-height spectral information from the multi-channel analyzer. The program moves the source to a specific location along the cathode, accumulates a pulse-height spectrum for a designated time (typically one-half hour), saves the spectrum, moves the source to the next location in the scan, and then repeats the process until a complete scan of a designated region is obtained. This results in the acquisition of a three-dimensional data set. Post-acquisition analysis software then allows various two-dimensional images to be formed from the three-dimensional data set. For example, a region of interest in the spectrum can be selected about the alpha-particle peak, and the peak centroid within this region can be calculated at each source location. This then generates a full-energy-peak centroid map of the scanned region of the crystal. Shifts in the peak location or peak smearing to lower energies will be reflected in the centroid map and thereby provide an image of the non-uniformities. These images can be then directly compared to other spatially mapped properties of the crystal in order to determine the possible cause of the spatial variations in electron generation and transport that are ultimately leading to the degraded gamma-ray detector performance.

After the alpha-particle scan of the crystal is complete, the source is then positioned at various locations of interest, and the induced charge signals are analyzed in detail. This typically consists of acquiring a set of induced charge pulses at the preamplifier output that have pulse heights spanning the range of the full-energy-peak width. From this set of pulses, the mechanisms that lead to peak broadening at that location or between different locations in the crystal may be evident. To see how this can be done, consider the sets of calculated induced charge signals plotted in Fig. 2. These signals were determined using the Hecht equation, which is valid during the electron drift:[28]

$$Q(t) = \frac{Q_o}{d} \mu_e E \tau_e \left(1 - e^{-t/\tau_e}\right). \quad (1)$$

In this equation Q is the magnitude of the charge induced on the detector anode, Q_o is the magnitude of the alpha-generated electron charge at the cathode, d is the detector length, E is the electric field magnitude in the detector, and μ_e and τ_e are the electron mobility and drift lifetime, respectively. It is assumed in this equation that the electron charge is generated at the detector cathode at a time of $t = 0$. Each panel in Fig. 2 consists of three superimposed charge pulses. The pulse with the largest height is the same for each panel and is calculated using typical values for the CdZnTe material and the measurement setup: $d = 1$ cm, $E = 1000$ V/cm, $\mu_e = 985$ cm^2/Vs, and $\tau_e = 5.1$ μs. The remaining two pulses in each panel were obtained by changing a particular material property to produce a 10 % and 20 % pulse height reduction. For example, in Fig. 2(a) the electron lifetime was reduced by 53 % and 71 % to produce pulse-height reductions of 10 % and 20 %, respectively. The increased curvature in the rise of these pulses is a direct result of the increased trapping and is an identifying feature of this type of variation. In Fig. 2(b), the product of the electron mobility and electric field was reduced by 53 % and 71 % to produce the pulse-height reductions. In this case, the variation is easily identified by the dramatic increase in the pulse rise time as caused by the slower electron velocity. Another example, shown in Fig. 2(c), is that of a localized trapping site where a variable amount of charge can be trapped. Here it was assumed that the trapping site was located at the midpoint of the crystal and that the fraction of the drifting charge trapped at the site was 21 % and 42 % for the two reduced height pulses. The reduction in the amount of drifting charge at the trapping site produces a distinctive reduction in slope of the signal rise. The final example, shown in Fig. 2(d), is that of a variation in the charge generated at the cathode. Since Q_o appears only as a prefactor in the induced charge signal equation, a fractional reduction in the generated charge directly produces the same fractional reduction in pulse height. These illustrative examples demonstrate that variations in certain material properties produce distinctive features in the induced charge signals. Through a careful analysis of these signals, it may be possible to determine the fundamental cause of the material non-uniformity leading to degraded gamma-ray detector performance.

Following the above analysis of the crystal in the planar detector configuration, the crystal is reprocessed into a coplanar-grid detector and tested. This allows us to directly correlate the characteristics measured through the alpha-particle analysis (and other characterization techniques) to the gamma-ray detector performance of the crystal. The fabrication procedure is similar to that of the planar detector, except that the full-area anode is replaced with a coplanar-grid electrode structure that is produced by performing the gold evaporation through a shadow mask. The coplanar-grid pattern was designed for charge induction uniformity using three-dimensional electrostatic modeling and then later tested for uniformity through alpha-particle scanning measurements.[15,16,18] The completed coplanar-grid detector is placed inside a test chamber where it is illuminated with gamma rays from a ^{137}Cs source and operated as a differential-gain coplanar-grid detector.[16] The operating conditions of the detector are then optimized in order to produce the best possible 662 keV gamma-ray peak resolution.

We end this section by summarizing the advantages and potential problems associated with the alpha-particle technique. The use of alpha particles to characterize the electron generation and transport of CdZnTe crystals provides several advantages. First, the 5.5 MeV alpha particles from the ^{241}Am source used in our measurements produce large signals and a well-defined energy deposition and interaction region (within 20 μm of the entrance contact electrode).[27] This small interaction region near the entrance contact enables the accurate characterization of the electron generation and collection properties. If instead, high-energy gamma rays were used, energy deposition will occur at random depths, which would introduce additional signal variations due to poor hole transport and lead to a less accurate characterization. A near-contact energy deposition could be achieved with a low-energy gamma-ray source. However, the resultant signal-to-noise level would be greatly reduced, and again, as a result, characterization accuracy would be degraded. A second advantage of alpha particles is that they are easily collimated and can therefore be used to probe small regions of the crystal. The source itself is also compact and easy to obtain, in contrast to accelerator-based sources of charged particles. Finally, the characterization procedure requires only a simple detector geometry and conventional pulse-processing electronics.

Despite the substantial advantages of the alpha-particle technique, some concerns need to be addressed. These relate to possible problems with electrical contact dead layers, obscured results from physical damage to the electrical contact, and charge loss due to recombination and trapping within the dense charge cloud created by an alpha particle. To address these concerns, we have conducted several experiments, all of which validate the use of the technique, at least for HPB CdZnTe material produced by eV Products and processed using the method described above. As reported previously,[24] the results of these experiments clearly indicate that the non-uniformity we observe using alpha-particles is due to bulk material effects, not contact or near-contact effects. However, it is important to note that the technique may not be as useful for other materials and/or fabrication processes. As an example, a cursory investigation of low-pressure Bridgman CdZnTe material obtained from Imarad Imaging Systems[29] revealed some problems. First, a crystal tested with indium contacts fabricated by Imarad produced anomalously large pulses with widely varying pulse heights when illuminated with alpha particles. One possible explanation for this is that trapped holes near the cathode lead to electron injection at that contact. These electrons do not necessarily recombine with the trapped holes because of the finite electron-hole recombination cross-section and the substantial applied field. These injected electrons can drift through the detector thereby resulting in a larger than expected pulse height. When an Imarad crystal was processed as described in this section, a contact thickness measurement gave an anomalous result.[24] A comparison of the collected charge from an alpha interaction event in that same crystal to that of a low-energy gamma ray indicated a significant charge collection deficit for the case of the alpha event. From these measurements, we conclude that the alpha characterization technique does not appear to be an appropriate tool to analyze the uniformity of this material, and a more appropriate choice might be low-energy gamma rays.

III. RESULTS

Alpha-particle scanning combined with pulse-height and induced-charge-signal analyses have proved useful for detailed investigations into the inhomogeneities of electron generation and transport in CdZnTe materials. In a previous study of HPB material,[23] we identified and mapped in three dimensions one type of non-uniformity, that of a variation in the product of electron mobility and electric field. Based on measurements and numerical modeling, we determined that a sufficiently large extent of such variations would degrade coplanar-grid detector performance and that such a level of this type of non-uniformity does exist in some crystals. These variations are readily identified through induced-charge-signal analysis. However, for the majority of the crystals that we have studied, the mobility-field variations observed are too small to account for the degraded coplanar-grid performance of the crystals. Non-uniformities apparently not explainable through simple mobility-field changes were also identified in previous studies.[23,24] The more severe of these were observed to have substantial variations over small length scales (less than 1 mm), and crystals with this problem were found to perform poorly as coplanar-grid detectors. In an effort to understand the nature of these and other non-uniformities, we have attempted to correlate the spatial dependence of the alpha response with spatial variations of other material properties. In this section, we present our findings from comparing alpha-particle response measurements to infrared transmission images of the crystals.

One approach to identify the dominant causes of spectroscopic performance degradation in CdZnTe materials is to analyze and compare crystals that have good coplanar-grid gamma-ray responses to those that perform poorly. Example measurements of this type are given in Figs. 3 and 4. Here the results from an identical set of measurements made on two separate crystals (labeled Crystal 1 and Crystal 2) are given. Plotted in part (a) of each figure is a full-area illumination alpha-particle spectrum acquired from the crystal when in a planar detector geometry. In part (b) of each figure, the coplanar-grid gamma-ray response of the crystal to a ^{137}Cs source is given. The alpha spectrum from Crystal 1 exhibits the desired single sharp full-energy peak with little background. As expected, this uniform crystal then achieves a good gamma-ray response as indicated by the 2.1 % FWHM energy resolution at 662 keV and the large peak-to-Compton ratio. In contrast to this is the response of Crystal 2. The alpha spectrum again consists of a single peak; however, this peak is broadened

thereby indicating a degraded material uniformity. This non-uniformity is then the likely cause of the mediocre gamma-ray response of the crystal.

The crystals that we have studied typically contain crystal defects such as pipes and tellurium precipitates or inclusions[25,30] that are identifiable through infrared transmission microscopy. One possible explanation for the poor uniformity in the detector response is that these defects either directly or indirectly affect charge generation or cause non-uniform electron trapping. To test this hypothesis and to better understand the performance degradation of Crystal 2, alpha-particle scans of Crystal 1 and Crystal 2 were taken. Part (c) of Figs. 3 and 4 contain the full-energy-peak centroid maps (in gray scale) extracted from these scans. Infrared images were also taken of the two crystals. The focal point of the infrared images was chosen to be near the cathode surface of the crystal, though, depending on object size, objects millimeters deep into the crystal can still be identified in the images. These infrared images were then processed to remove any slowly varying background and then converted to binary images by choosing a threshold level that selects out the majority of in-focus objects in the images. For presentation purposes, these objects (black) were then expanded in size and outlined in white. The resultant processed infrared images are plotted as an overlay on the alpha-peak centroid maps in Figs. 3(c) and 4(c). The array of gray pixels in each figure is the centroid map, and the black objects outlined in white are the regions of low infrared transmission. As a first observation, note that the centroid map of Crystal 1 shows that the response of the crystal is relatively uniform over most of the scanned area with centroid variations of only about 1 %. The map of Crystal 2 in contrast is clearly less uniform and contains variations of about 2 % in the centroid position over distances of less than 1 mm. This reaffirms the idea that the loss of gamma-ray spectral performance is a direct result of a lack of uniformity in electron generation and/or transport as identified through alpha-particle response measurements.

A second observation from Figs. 3(c) and 4(c) is that there is a clear correlation between the presence of certain defects identified through infrared microscopy and reduced alpha-peak centroid. Crystal 1 is relatively free from identified defects and perhaps as a result has a relatively uniform alpha response. The objects in the form of horizontal lines in the infrared image are pipes. It is not clear what influence these pipes have on the uniformity of the detector response. The pipe segments at y positions of 2.2 mm, -0.7 mm, and -1.2 mm appear to have little effect on the alpha-peak centroid. Respectively, these pipes are approximately 5.5 mm, 0 mm, and 8 mm deep into the crystal from the cathode surface. On the other hand, two pipes at the y position of -2 mm (2 mm and 3 mm deep into the crystal) are associated with regions of reduced centroid in the alpha response map. Induced charge signals (not shown) acquired at the alpha source locations of x = 0.9 mm and y = -1.9 mm indicate that the reduced centroid is a result of a variable amount of electron trapping taking place at a depth in the crystal corresponding to the location of the pipes. The effects of these pipes however are confined to a small fraction of the total area of the detector and therefore do not significantly degrade the spectral performance.

The infrared image of Crystal 2 indicates that, unlike Crystal 1, Crystal 2 contains numerous defects approximately 20 - 30 μm in diameter dispersed throughout the crystal. These objects are most likely the often-identified tellurium inclusions found in CdZnTe materials. The data of Fig. 4(c) indicate that there is a reasonably good correlation between the inclusion locations and areas with reduced centroid of the alpha peak. This correlation has also been observed in other similar crystals. A comparison of the data obtained from a region free from inclusions (labeled a1 in Fig. 4(c)) to that of a region with a large number of inclusions (labeled a2 in Fig. 4(c)) is shown in Fig. 5. From the pulse-height spectra of Fig. 5(a), we see that the region free from inclusions (a1) exhibits a single sharp full-energy peak thereby indicating good uniformity in the small area probed by the alpha beam. In contrast, the region containing many inclusions (a2) produces a peak that is broadened to lower energies. This broadening rather than a simple peak shift is the cause of the reduced centroid observed in the Fig. 4(c) map. It is not clear if the inclusions themselves are responsible for the degradation or if they are just spatially associated with other material defects that affect the detector signal. However, we can conclude that the degradation effects are correlated with the location of the inclusions, and the effects extend beyond the physical volume occupied by the inclusions. To see this, realize that the alpha-particle probe beam is approximately 300 μm in diameter while the diameter of the larger inclusions is only about 30 μm. If even several of these inclusions are contained within the alpha beam, the fraction of the beam area occupied by inclusions will still be less than 10 %. We see from Fig. 5(a) that the reduced centroid is due to a large fraction of the counts being shifted to lower energies. This indicates that a large fraction of the alpha events is affected. Therefore, the degraded region of the crystal must be larger than the cross-sectional area of the inclusions.

In an effort to determine the mechanism given rise to the non-uniformity seen in Crystal 2, we have analyzed the induced charge signals that result when various regions are probed with alpha particles. Example pulses acquired at locations a1 and a2 are shown in Figs. 5(b) and 5(c), respectively. As expected there is not much variation in the pulses associated with the region free from inclusions. The signals acquired at the location with many inclusions, in contrast, appear to diverge from each other very near the start of the electron drift process (near the cathode). This set of induced charge signals is similar to the calculated ones of Fig. 2(d) for the case of a variation in the charge generated by each alpha-particle interaction event. However, a similar set of signals could also be produced by the mechanism shown in Fig. 2(c) if the trapping site was located near the cathode. Therefore, from these data alone it is unclear if the non-uniform response of Crystal 2 is due to variations in charge generation or variations in electron trapping near the cathode. An interesting observation is that the

alpha centroid map of Crystal 2 correlates well with the infrared transmission image when the camera focus is set near the cathode surface of the crystal. The image obtained with the focus set near the anode (not shown) does not correlate well. In other words, the alpha scan appears to correlate only with the lateral distribution of inclusions near the surface of the crystal where the alpha particles enter the crystal. This may initially lead one to believe that the presence of inclusions somehow affects the amount of charge generated by the alpha particles, which then gives rise to the signal variation. However, non-uniform electron trapping is also a possible mechanism since its effect on the alpha particle signals is most pronounced when the trapping sites are near the cathode. This is illustrated in Fig. 6 where we plot the calculated pulse height deficit or reduction due to a site of enhanced electron trapping as a function of the site's distance from the cathode. As is intuitively expected, when charge is trapped near the start of the electron drift process (trapping site near the cathode), the resultant pulse-height deficit is greater. Consequently, the two degradation mechanisms of variations in charge generation and sites of enhanced electron trapping distributed throughout the crystal volume will both produce alpha responses that are particularly dependent on the material characteristics near the cathode of the crystal.

To determine if the observed degradation is due to variations in charge generation or trapping, we have performed detailed alpha response measurements on a crystal (designated Crystal 3) with larger though fewer inclusions than that of Crystal 2. Alpha-particle scanning and infrared transmission microscopy measurements identical to those made on Crystals 1 and 2 were made on Crystal 3. The results are shown in Fig. 7. As with Crystal 2, there is a clear correlation between inclusion location and reduced alpha-peak centroid in the data from Crystal 3. However, the more sparse distribution of inclusions in this crystal has allowed us to measure the degradation associated with single inclusions. The locations of the inclusions in Crystal 3 were not only determined in the lateral dimensions of x and y but also in the depth dimension of z using infrared microscopy. Based on this information, locations near a single relatively isolated inclusion were probed with the alpha beam, and induced charge signals were acquired. Four of these locations are identified in Fig. 7 as b1 through b4, and the associated induced charge signals are given in Fig. 8. Also shown with an arrow in each panel of Fig. 8 is the calculated time at which the drifting electrons passed by the inclusion. This was determined using the electron drift time from the induced charge signals and the inclusion depth from the infrared microscopy measurements, and by assuming that the electrons drift at a constant velocity. The results obtained at each location are similar in that the signals at a particular location are nearly identical to each other until the time at which the electrons drift near the inclusion. Near the inclusion, a variable amount of additional electron trapping takes place (similar to the calculated signals of Fig. 2(c)). This then produces a divergence in the signals and ultimately a variation in the pulse heights. We therefore conclude that the basic mechanism for the non-uniform detector response is enhanced electron trapping at localized regions associated with the inclusions.

A schematic representation of the process leading to electron transport non-uniformity in these crystals with relatively large inclusions is depicted in Fig. 9. Two separate alpha-particle interaction events originating from the same beam are shown. In the first, the electron charge drifts through a region free of inclusions and experiences uniform electron trapping throughout the charge collection process. The second event in contrast results in electrons that drift within the enhanced trapping regions associated with inclusions and therefore suffer from additional trapping. These two events will then produce different pulse-heights in the detection electronics. Events occurring randomly at different locations will then give different pulse heights. Therefore, the spectroscopic performance of the detector will be degraded. This appears to be the dominant mechanism affecting the detector performance in several crystals that we have studied that contain relatively large inclusions (diameters greater than about 20 μm). At this point, it is unclear as to the specific defects that produce the enhanced trapping regions surrounding the inclusions. It is reasonable, though, that the additional trapping is the direct result of dislocation fields that have been observed surrounding inclusions in CdZnTe material.[25]

IV. SUMMARY

The successful application of simple electron-only devices for high-resolution spectroscopy requires detector material that is highly uniform in both electron generation and transport. Our measurements illustrate that the degree of non-uniformity that affects detector performance can be at the 1% level. Consequently, any useful characterization and analysis technique must be sensitive down to this level. We have shown that alpha-particle response measurements are capable of directly characterizing electron generation and transport uniformity at the required accuracy. Through alpha-particle scanning combined with pulse-height and induced-charge-signal analyses, we have made detailed studies of the non-uniformities present in CdZnTe crystals that are free from random grain boundaries. From these and other studies, it is clear that multiple mechanisms play roles in the degradation of the gamma-ray performance of such crystals. For some crystals, we have observed a clear correlation between non-uniformities in electron generation and transport, and the distribution of large tellurium inclusions in the crystals. These non-uniformities are most likely the dominant effect degrading the gamma-ray performance of these crystals. From a geometry argument, we conclude that the region of degraded performance near an inclusion extends beyond the volume of the inclusion itself. From induced charge signal measurements, we see that this degradation is in the form of enhanced electron trapping.

ACKNOWLEDGMENTS

This work was supported by the Office of Defense Nuclear Nonproliferation, Office of Nonproliferation Research and Engineering (NA-22), of the U.S. Department of Energy under Contract No. DE-AC03-76SF00098.

REFERENCES

[1] Semiconductors for Room Temperature Nuclear Detector Applications, edited by T. E. Schlesinger and R. B. James, Semiconductors and Semimetals **43** (Academic Press, New York, 1995) and references therein.
[2] Y. Eisen and A. Shor, J. Crystal Growth **184/185**, 1302 (1998), and references therein.
[3] T. E. Schlesinger, J. E. Toney, H. Yoon, E. Y. Lee, B. A. Brunett, L. Franks, and R. B. James, Mat. Sci. Eng. **32**, 103, (2001), and references therein.
[4] P. N. Luke, Appl. Phys. Lett. **65**, 2884 (1994).
[5] P. N. Luke, IEEE Trans. Nucl. Sci. **42**, 207 (1995).
[6] H. H. Barrett, J. D. Eskin, and H. B. Barber, Phys. Rev. Lett. **75**, 156 (1995).
[7] Z. He, G. F. Knoll, D. K. Wehe, R. Rojeski, C. H. Mastrangelo, M. Hammig, C. Barrett, and A. Uritani, Nucl. Instr. Meth. Phys. Res. **A380**, 228 (1996).
[8] M. Amman and P. N. Luke, Proc. of SPIE **3115**, 205 (1997).
[9] Z. He, G. F. Knoll, D. K. Wehe, and J. Miyamoto, Nucl. Instr. Meth. Phys. Res. **A388**, 180 (1997).
[10] D. S. McGregor, Z. He, H. A. Seifert, D. K. Wehe, and R. A. Rojeski, Appl. Phys. Lett. **72**, 792 (1998).
[11] Z. He, W. Li, G. F. Knoll, D. K. Wehe, J. Berry, C. M. Stahle, Nucl. Instr. Meth. Phys. Res. **A422**, 173 (1999).
[12] M. Mayer, L. A. Hamel, O. Tousignant, J. R. Macri, J. M. Ryan, M. L. McConnell, V. T. Jordanov, J. F. Butler, and C. L. Lingren, Nucl. Instr. Meth. Phys. Res. **A422**, 190 (1999).
[13] P. N. Luke, M. Amman, J. S. Lee, and H. Yaver, Nucl. Instr. Meth. Phys. Res. **A439**, 611 (2000).
[14] C. Szeles and M. C. Driver, Proc. of SPIE **3446**, 2 (1998).
[15] P. N. Luke, M. Amman, T. H. Prettyman, P. A. Russo, and D. A. Close, IEEE Trans. Nucl. Sci. **44**, 713 (1997).
[16] M. Amman and P. N. Luke, IEEE Trans. Nucl. Sci. **46**, 205 (1999).
[17] T. H. Prettyman, M. K. Smith, and S. E. Soldner, Proc. of SPIE **3768**, 339 (1999).
[18] P. N. Luke, M. Amman, J. S. Lee, B. A. Ludewigt, and H. Yaver, Nucl. Instr. Meth. Phys. Res. **A458**, 319 (2001).
[19] P. N. Luke and E. E. Eissler, IEEE Trans. Nucl. Sci., **43**, 1481 (1996).
[20] F. P. Doty, J. P. Cozzatti, and J. P. Schomer, Proc. of SPIE **3115**, 51 (1997).
[21] B. H. Parker, C. M. Stahle, S. D. Barthelmy, A. M. Parsons, J. Tueller, J. T. Van Sant, B. F. Munoz, S. J. Snodgrass, and R. E. Mullinix, Proc. of SPIE **3768**, 129 (1999).
[22] M. Amman, J. S. Lee, and P. N. Luke, Proc. of SPIE **3446**, 179 (1998).
[23] M. Amman, P. N. Luke, and J. S. Lee, IEEE Trans. Nucl. Sci. **47**, 760 (2000).
[24] M. Amman, J. S. Lee, and P. N. Luke, Proc. of SPIE **4507**, 1 (2001).
[25] C. Szeles, W. C. Chalmers, S. E. Cameron, J. Ndap, M. Bliss, and K. G. Lynn, Proc. of SPIE **4507**, 57 (2001).
[26] eV Products, a division of II-VI, Inc., Saxonburg, PA 16056.
[27] SRIM program described in The Stopping and Range of Ions in Solids, J. F. Ziegler, J. P. Biersack, and U. Littmark, (Pergamon Press, New York, 1985).
[28] K. Hecht, Z. Phys. **77**, 235 (1932).
[29] Imarad Imaging Systems Ltd., Rehovot, Israel.
[30] R. B. James, B. Brunett, J. Heffelfinger, J. Van Scyoc, J. Lund, F. P. Doty, C. L. Lingren, R. Olsen, E. Cross, H. Hermon, H. Yoon, N. Hilton, M. Schieber, E. Y. Lee, J. Toney, T. E. Schlesinger, M. Goorsky, W. Yao, H. Chen, and A. Burger, J. Electr. Mat. **27**, 788 (1998).

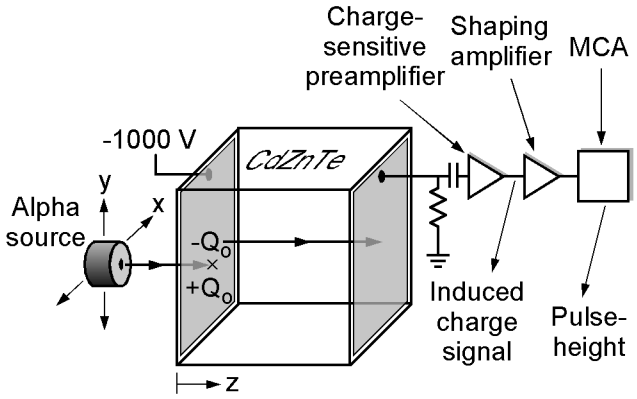

FIG. 1. Schematic diagram of the alpha-particle response measurement configuration used to study the uniformity of electron generation and transport in CdZnTe crystals. In this technique, the crystal is fabricated into a planar detector, a bias is applied, and the detector cathode is probed with alpha particles. Induced charge signals resultant from the collection of alpha-generated electrons are then analyzed directly or through pulse-height analysis.

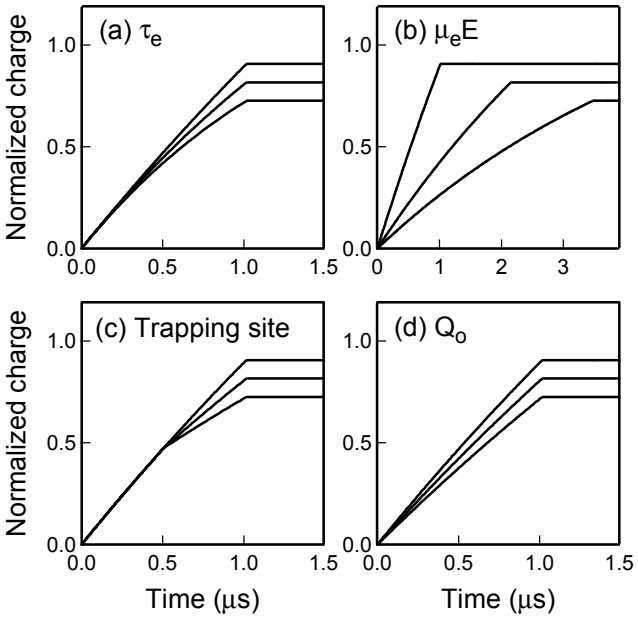

FIG. 2. Superimposed calculated induced charge signals from a charge-sensitive preamplifier connected to the anode of a planar CdZnTe detector. The detector was assumed to have a length of 1 cm and an applied bias of 1000 V. Each signal results from the collection of electron charge generated by an alpha-particle interaction event at the cathode of the detector. In each panel, the pulse with the largest height was determined using typical transport properties for CdZnTe. The other pulses were determined by adjusting the following properties to produce a 10 % and a 20 % pulse-height reduction: (a) electron lifetime, (b) product of electron mobility and electric field, (c) trapping fraction at a trapping site, and (d) quantity of electron charge generated at the cathode.

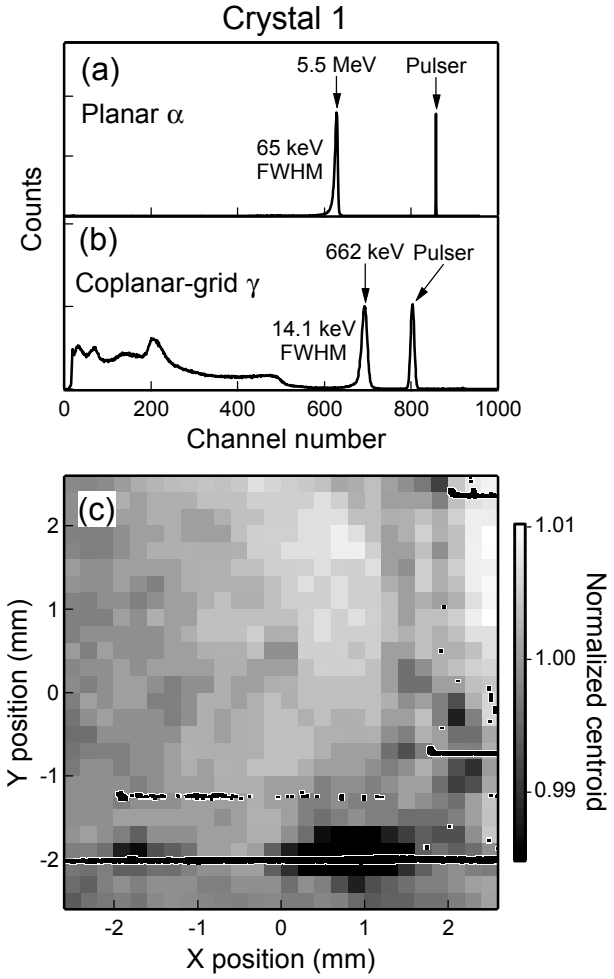

FIG. 3. Measurements from the relatively uniform CdZnTe Crystal 1. (a) ^{241}Am alpha-particle pulse-height spectrum obtained with the crystal in a planar detector geometry. The detector bias was 1000 V. The source was uncollimated and illuminated the full cathode area of the crystal. (b) ^{137}Cs gamma-ray pulse-height spectrum obtained with the crystal in a coplanar-grid detector geometry. The bias across the detector was 1400 V and that between the grids was 39 V. The 662 keV gamma-ray peak to Compton ratio for this spectrum is 6.2. (c) Alpha-particle-peak centroid image of the center section of the crystal. An ^{241}Am alpha source collimated to about 300 μm was used to scan the cathode side of the crystal in a planar detector configuration while a bias of 1000 V was applied across the detector. Superimposed on top of this image are regions (black with white outline) of low infrared transmission.

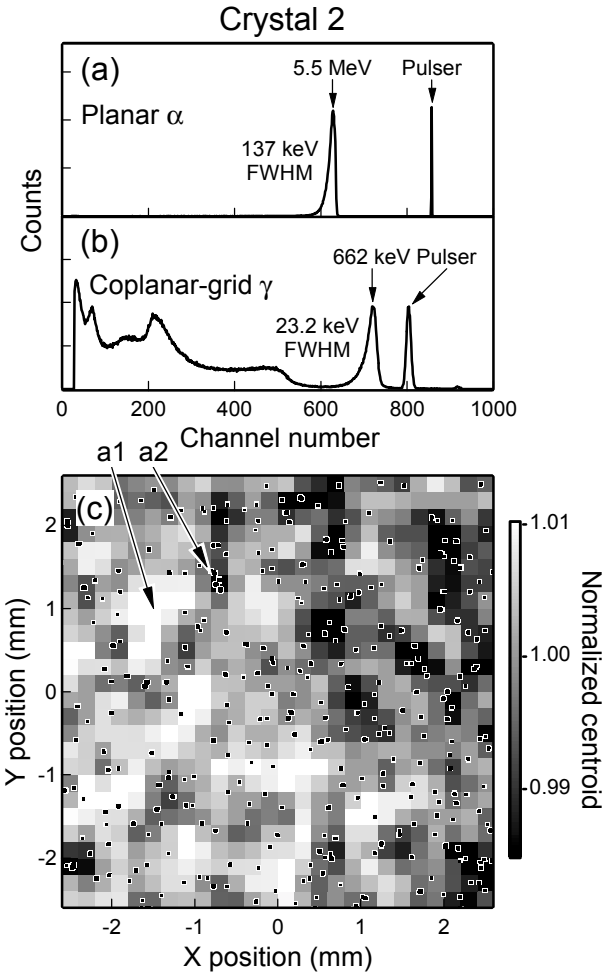

FIG. 4. Measurements from the relatively non-uniform CdZnTe Crystal 2. (a) ^{241}Am alpha-particle pulse-height spectrum obtained with the crystal in a planar detector geometry. The detector bias was 1000 V. The source was uncollimated and illuminated the full cathode area of the crystal. (b) ^{137}Cs gamma-ray pulse-height spectrum obtained with the crystal in a coplanar-grid detector geometry. The bias across the detector was 1600 V and that between the grids was 65 V. The 662 keV gamma-ray peak to Compton ratio for this spectrum is 3.9. (c) Alpha-particle-peak centroid image of the center section of the crystal. An ^{241}Am alpha source collimated to about 300 μm was used to scan the cathode side of the crystal in a planar detector configuration while a bias of 1000 V was applied across the detector. Superimposed on top of this image are regions (black with white outline) of low infrared transmission.

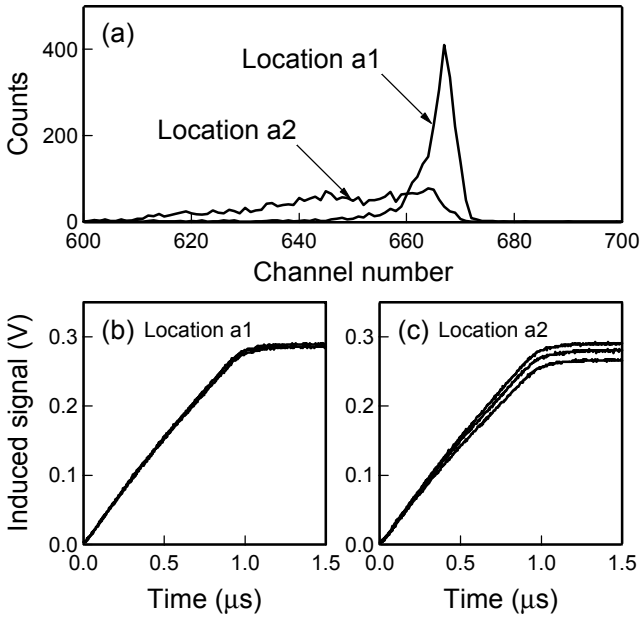

FIG. 5. (a) Superimposed alpha-particle pulse-height spectra obtained at the source locations indicated in Fig. 4(c) for Crystal 2. (b) Superimposed induced charge signals measured with the alpha-particle source at location a1. (c) Superimposed induced charge signals measured with the alpha-particle source at location a2.

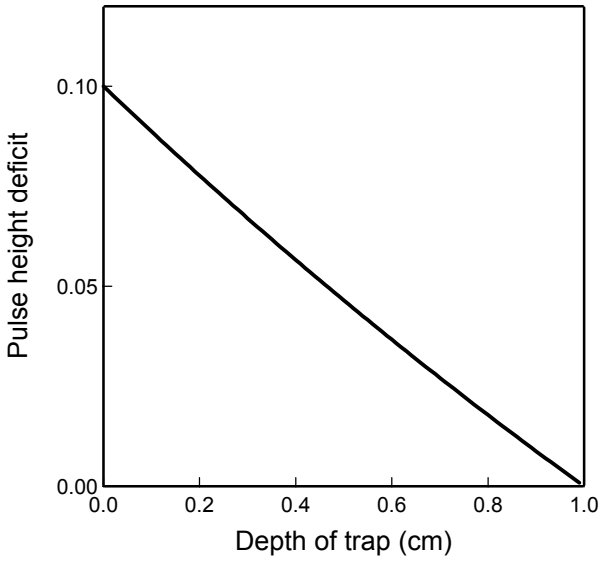

FIG. 6. Calculated pulse-height reduction resulting from a trapping site located along the drift path of electron charge being collected from the cathode to the anode of a planar CdZnTe detector. The pulse signal is the induced charge signal measured by a charge-sensitive preamplifier connected to the anode of the detector. The fractional reduction in the pulse-height relative to the pulse height with no trapping site is plotted as a function of the trapping site location. The detector was assumed to be 1 cm in length with 1000 V applied, and the properties of the CdZnTe were those measured from Crystal 2: μ_e = 934 cm^2/Vs and τ_e = 3.8 μs. It was also assumed that 10 % of the drifting charge was trapped by the trapping site.

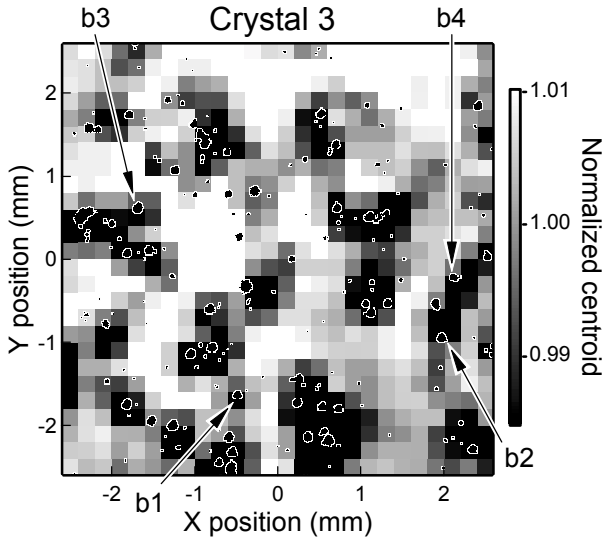

FIG. 7. Alpha-particle-peak centroid image of the center section of the relatively non-uniform CdZnTe Crystal 3. An ^{241}Am alpha source collimated to about 300 μm was used to scan the cathode side of the crystal in a planar detector configuration while a bias of 1000 V was applied across the detector. Superimposed on top of this image are regions (black with white outline) of low infrared transmission.

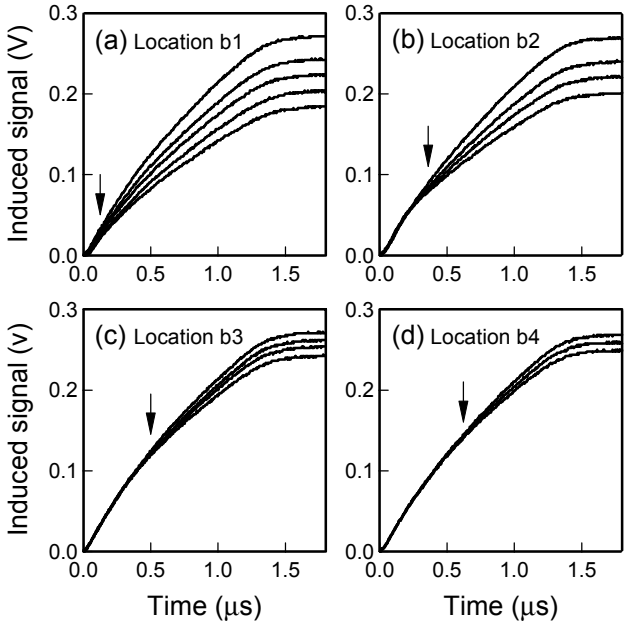

FIG. 8. Superimposed induced charge signals measured at the alpha-particle source locations indicated in Fig. 7 for Crystal 3. Each source location corresponds to the lateral location of a single inclusion whose depth within the crystal was determined through infrared microscopy. The calculated time at which the drifting electrons passed the inclusion is indicated in each panel of the figure with an arrow. At this time in the drift process there was apparently some additional electron trapping that took place. This trapping then resulted in a substantial variation between the pulses at each location.

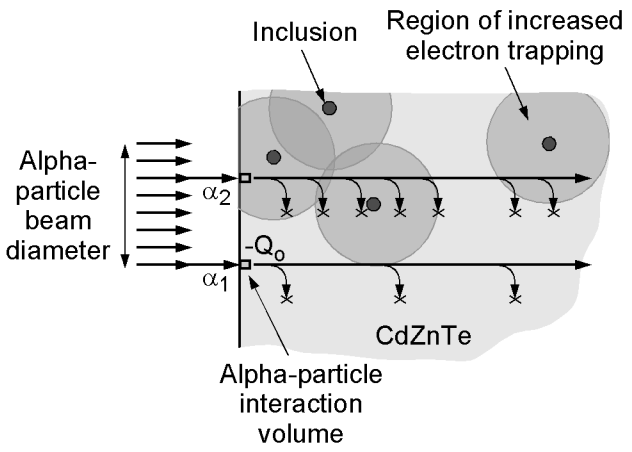

FIG. 9. Schematic diagram to explain the non-uniformity in electron transport of the CdZnTe crystals described in this paper. Associated with the tellurium inclusions in the crystal are regions of increased electron trapping. This spatially non-uniform electron trapping produces induced charge signal variations in the alpha-particle response measurements and, ultimately, degrades gamma-ray detector performance.